Supporting Information

The making of natural iron sulfide nanoparticles in a hot vent snail

Satoshi Okada[a,1], Chong Chen[b], Tomo-o Watsuji[c], Manabu Nishizawa[b], Yohey Suzuki[d], Yuji Sano[e, f], Dass Bissessur[g], Shigeru Deguchi[a], Ken Takai[b]

[a] Research Center for Bioscience and Nanoscience (CeBN), Research Institute for Marine Resources Utilization, Japan Agency for Marine-Earth Science and Technology (JAMSTEC), 2-15 Natsushima-cho, Yokosuka, Kanagawa 237-0061, Japan.

[b] Institute for Extra-cutting-edge Science and Technology Avant-garde Research (X-star), Japan Agency for Marine-Earth Science and Technology (JAMSTEC), 2-15 Natsushima-cho, Yokosuka, Kanagawa 237-0061, Japan.

[c] Department of Food and Nutrition, Higashi-Chikushi Junior College, 5-1-1 Shimoitouzu, Kitakyusyu, Fukuoka 803-0846, Japan.

[d] Department of Earth and Planetary Science, Graduate School of Science, The University of Tokyo, 7-3-1 Hongo Bunkyo-ku, Tokyo 113-0033, Japan

[e] Department of Chemical Oceanography, Atmosphere and Ocean Research Institute, The University of Tokyo, 5-1-5 Kashiwa-no-ha, Kashiwa, Chiba 277-8564, Japan.

[f] Institute of Surface-Earth System Science, Tianjin University, 92 Weijin Road, 18 Nankai District, Tianjin, 300072, P.R. China.

[g] Department for Continental Shelf, Maritime Zones Administration & Exploration, Ministry of Defence and Rodrigues, 2nd Floor, Belmont House, 12 Intendance Street, Port-Louis 11328, Mauritius.

Methods

Nano-SIMS analysis of scales

For isotopic analysis, two pieces of sclerite samples of black scaly-foot collected during YK01-15 cruise were embedded in Spurr's epoxy resin (Polysciences, Inc.). The mounted samples were polished by sheets with alumina grains and then 1 μm diamond paste. Finally, the polished surface was gold-coated to dissipate charge during analysis.

The *in situ* S isotopic analysis of pyrite in sclerites was performed by the high mass resolution (HMR) method using the double-focusing ion microprobe at the Atmosphere and Ocean Research Institute, The University of Tokyo (NanoSIMS NS50, CAMECA, France) (1). 900 μm^2 (30 × 30 μm) domains within the sample was pre-sputtered by a primary beam of 500 pA Cs^+ (16 keV) for 180 s in raster mode before isotope measurement. Then, a primary beam of 8 pA Cs^+ (16 keV) was focused onto a small spot (3 μm in diameter) within the domain. Electron flood gun for charge compensation was not used. The $^{32}S^-$ and $^{34}S^-$ ions were measured simultaneously for 200 s using Faraday cup and electron multiplier pulse counting detectors, respectively. Mass resolutions of 3000 and 3100 at 1% peak heights were attained for the $^{32}S^-$ and $^{34}S^-$ ions, respectively. No isobaric interferences were observed for these ions in a pyrite matrix. Typical intensities of $^{32}S^-$ and $^{34}S^-$ ions are 540 femtoampere, which is equivalent to 3.4×10^5 counts per second (cps), and 1.5×10^5 cps, respectively. To correct any effects of mass bias, the $^{34}S^-/^{32}S^-$ ratio of the laboratory reference pyrite from ore deposits (73092809) was measured repeatedly at the beginning, during and end of analytical session. S isotopic data are referenced to the Vienna-Canyon Diablo Troilite (VCDT) scale and are reported using delta notation: $\delta^{34}S = (^{34}R_{sample}/^{34}R_{VCDT} - 1) \times 1000$, where $^{34}R_{sample}$ denotes $^{34}S/^{32}S$ ratio of pyrite in sclerite.

Sample preparation for electron microscopy

A scale was fixed on a φ12.5 × 10 mm brass stub or φ10 × 10 mm aluminum stub using carbon paste (Nisshin EM) and observed the surface structure without further coating.

Two pieces of the scales for cross-section analysis were embedded in epoxy resin (TAAB) following the Luft's method(2). The resin blocks were polished using silicon carbide grinding papers #320, 600, 800, 4000, and 7-μm diamond slurry until the cross section of scales appeared (Ecomet III, Buehler) and then sliced to 100–500 nm by an ultramicrotome (Ultracut S or EM UC7, Leica) mounted with a SYM knife (45°, Syntek) in a longitudinal direction. The thin-sections were collected on Rh-coated Cu grids (100 mesh, Nisshin EM Co., Ltd.) with formvar from 1% chloroform solution after hydrophilization (DII-29020HD, JEOL).

Electron microscopic observation

SEM/STEM observations with EDS analyses were performed either on Helios G4 UX (Thermo Fisher Scientific, equipped with Octane Elite Super EDS detector, AMETEK) or on Quanta 450 FEG (Thermo Fisher Scientific, equipped with Octane Elite EDS detector, AMETEK) operated at 25 kV. TEM/STEM observations with EDS analyses were performed on Tecnai G2 20 (Thermo Fisher Scientific, operated at 120 or 200 kV) equipped with a bottom-mounted 2k × 2k Eagle CCD camera (Thermo Fisher Scientific) and RTEM-S 61700ME EDS detector (AMETEK). The approximate positions of the electron microscopic images are summarized in SI Appendix, Fig. S1.

Image analysis

Obtained SEM images were either manually segmented using Affinity Photo for iPad 1.6.8.77 (Serif (Europe) Ltd.) and then analyzed in Image-Pro 3D v9.3 (Media Cybernetics, for $N < 1000$), or directly analyzed in Image-Pro 3D. The particle sizes reported are in average (diameter) ± standard deviation. The inter-column distance was calculated based on the area of Voronoi diagram in Image-Pro 3D. For visuality, contrast and

brightness of STEM/EDS mapping images were modified.

Three-dimensional imaging

A black scaly-foot scale embedded in epoxy resin while exposing a cross section along the longitudinal direction was coated with carbon three times (CADE, Meiwafosis, operated at 6 Pa). The resin block was imaged on Helios G4 UX equipped with a gallium ion beam. FIB-SEM images were automatically acquired using the Auto Slice & View software (version 4.0.3.846, Thermo Fisher Scientific) at the acceleration voltage of 3 kV and the voxel size of 4.1 × 4.1 × 15 nm using the mirror detector that collects the backscattered electron. Obtained serial sections were processed on the specialist 3D software Amira 2019.2 (Thermo Fisher Scientific).

Microscopic infrared spectroscopy imaging

Microscopic infrared spectroscopy imaging was performed on an IRT-7000 equipped with FTIR-6200 (JASCO). Cross sections of the scales were prepared by slicing the epoxy-embedded blocks used for electron microscopic analysis to 1 μm thickness using an ultramicrotome (EM UC7, Leica) mounted with a Histo knife (45°, DiATOME) in a longitudinal direction. The semi-thin sections were collected on Rh-coated Cu grids (100 mesh, Nisshin EM Co., Ltd.) with formvar from 1% chloroform solution after hydrophilization (DII-29020HD, JEOL). The grid was placed on a CaF_2 plate (ϕ 13 mm × 1 mm) and spectrum was acquired at the aperture size of 50 × 15 μm. As shown in the spectra, metallic grid and the amorphous carbon film does not affect the spectral region of 1500–1800 cm^{-1} concerned in this study.

pH analysis of white scaly-foot body fluids

Three individuals of the white scaly-foot frozen in –80°C (same collection data as above) was dissected to isolate the blood circulation system, the esophageal gland where

the endosymbionts are located, and the foot at room temperature. The body fluids were collected by squeezing the separated blood circulation system, esophageal gland with bacteria, and the foot muscle. The pH of the fluids were measured on a pH meter (LAQUAtwin-pH-22B, Horiba, calibrated at pH 4.01 and 6.86) after temperature equilibration for more than an hour. The temperature was monitored on a digital thermometer equipped with a thermocouple type K (CENTER 520, MK scientific, Inc.).

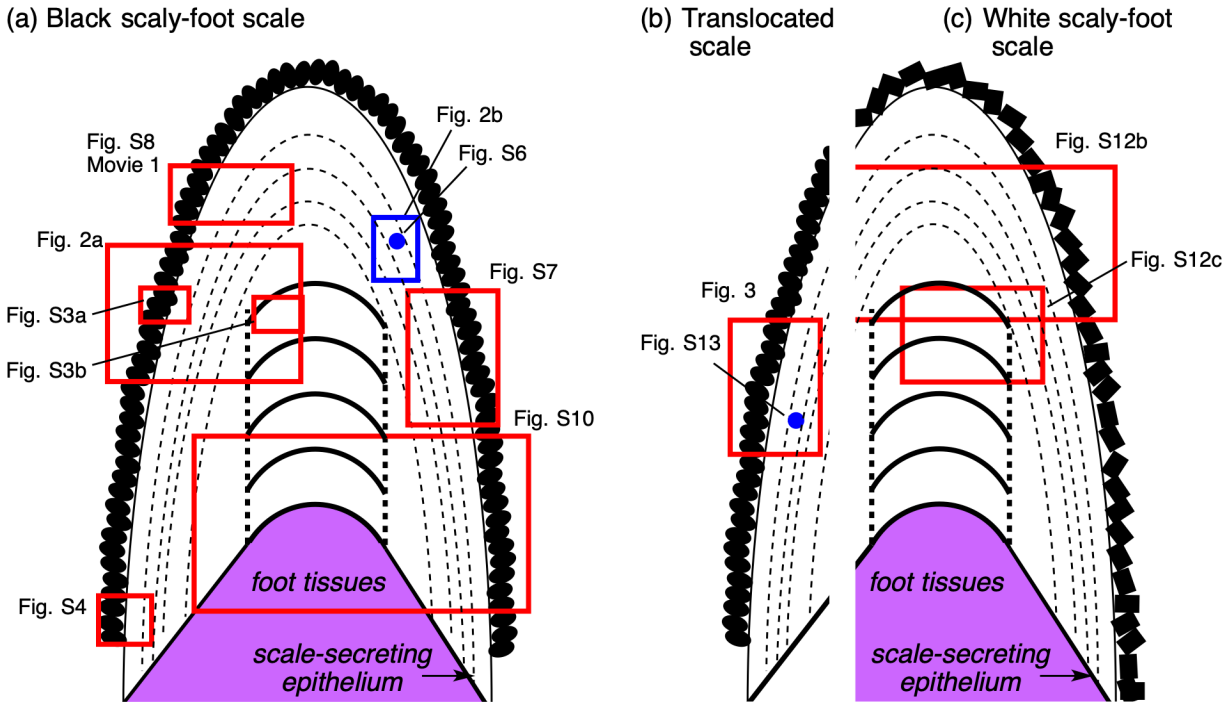

Figure S1. Approximate positions of the electron microscopic images in the figures. (a) Black scaly-foot scale with foot tissue, (b) translocated scale, and (c) white scaly-foot scale. Red colored area represent positions of SEM/STEM images taken at 25 kV and blue colored area show that of TEM/STEM images taken at 120 or 200 kV. Images are not to scale and do not represent the relative positions between images, as several sections were observed. The solid black layer on the outside represents the Outermost layer, thin dotted lines represent the Middle layer, while the thicker dotted lines in the middle represents the Innermost layer. Also see Fig. 1b in the reference (3) for an optical micrograph showing the scale-epithelium interface.

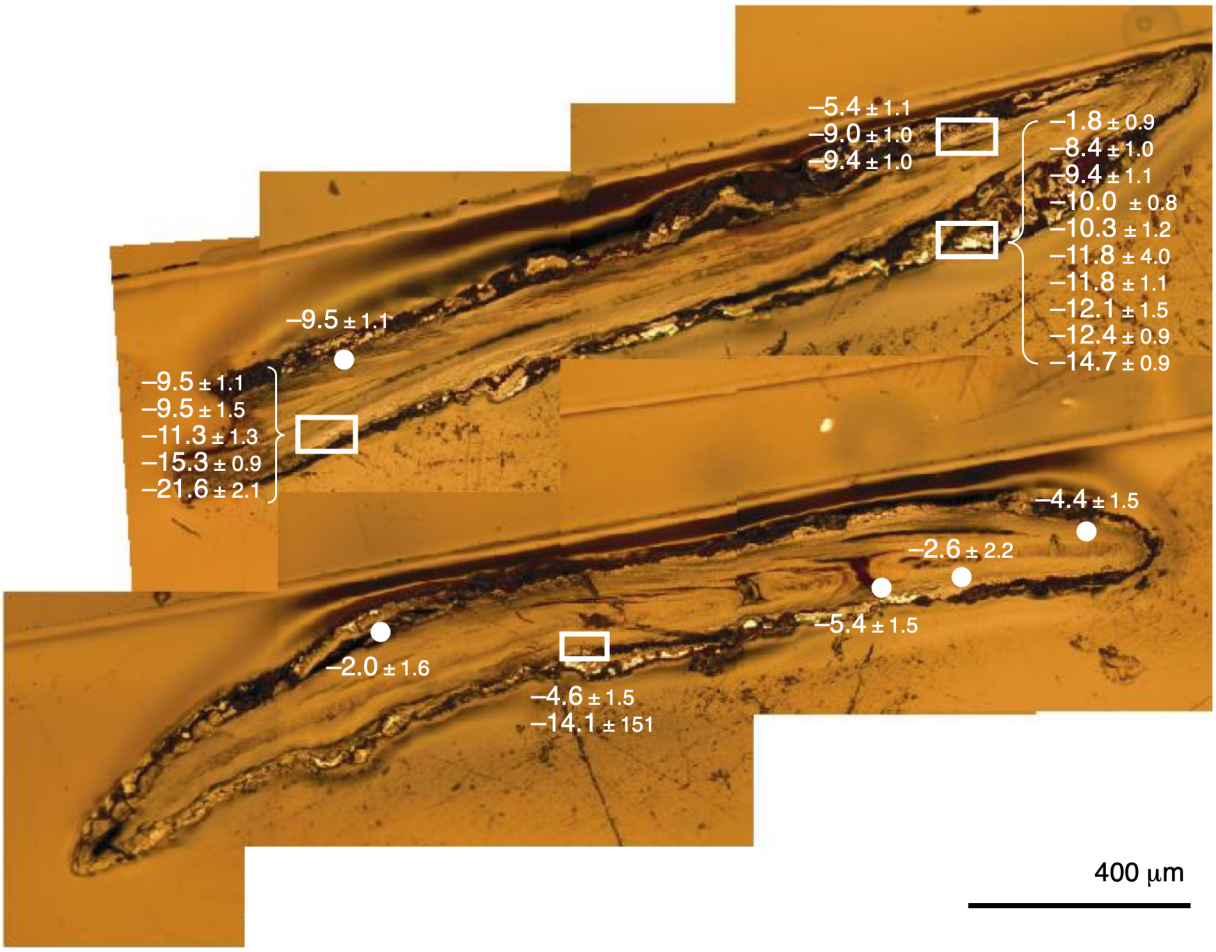

Figure S2. Nano-SIMS analysis of cross-section of black scaly-foot scales. Analyzed areas are shown in white dots (single point) and squares (multiple points) on image montages of optical microscopy. $\delta^{34}S$ value in ‰ referenced to the Vienna-Canyon Diablo Troilite (VCDT) scale are shown in photograph.

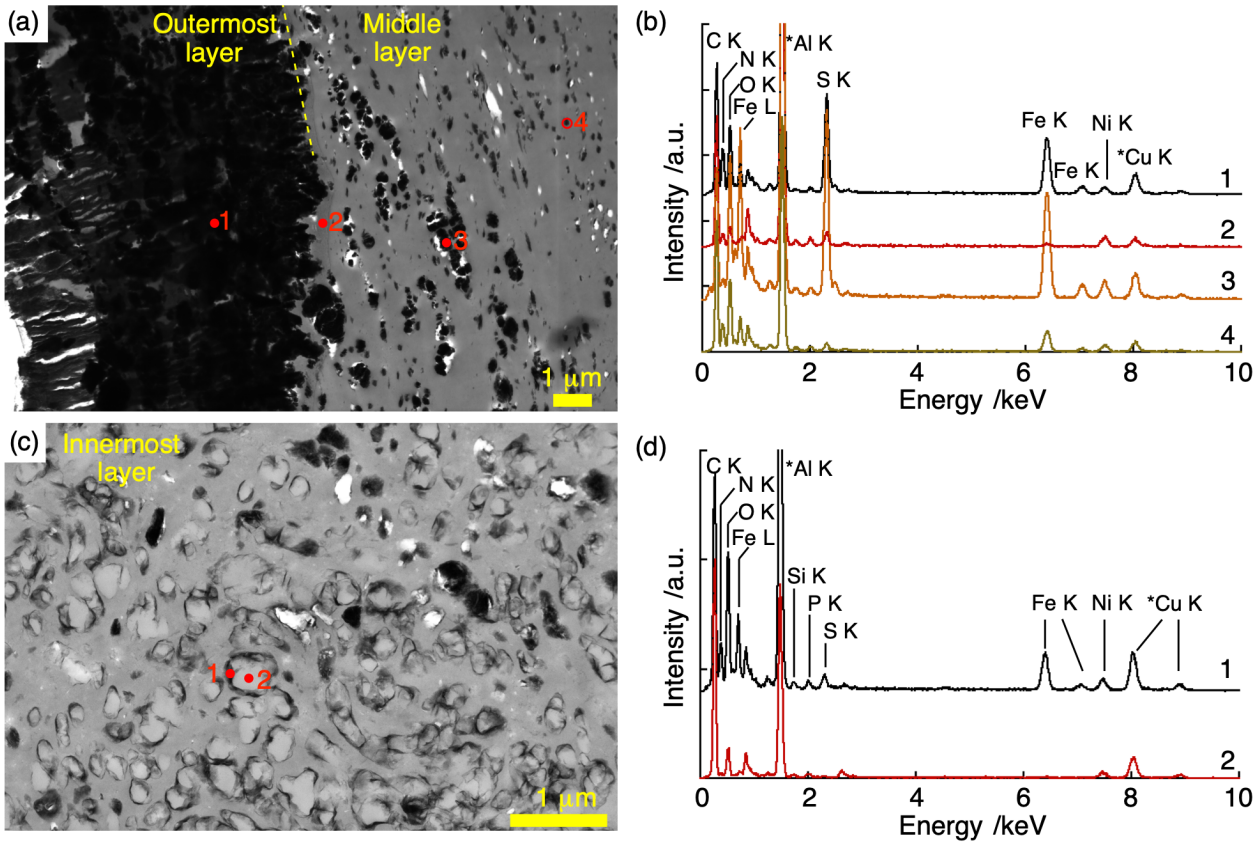

Figure S3. Cross-sectional bright-field STEM images of the black scaly-foot scale. (a) High-magnification images of the outermost and middle layers. **(b)** EDS analyses of the red dotted positions in (a). Position 1, minerals in the outermost layer; position 2, non-mineralized scale in the middle layer; position 3, aggregated mineral particles in the middle layer; position 4, small mineral particles in the middle layer. The elemental composition is summarized in Table S2. **(c)** High-magnification images of the innermost layer. **(d)** EDS analyses of the red dotted positions in (a). Position 1, minerals in the innermost layer; position 2, non-mineralized scale in the innermost layer. The elemental composition is summarized in Table S3. Images and spectra were taken at 25 kV. Note that Al, Si and Cu originates from microscopic chamber, STEM detector, and specimen grid, respectively.

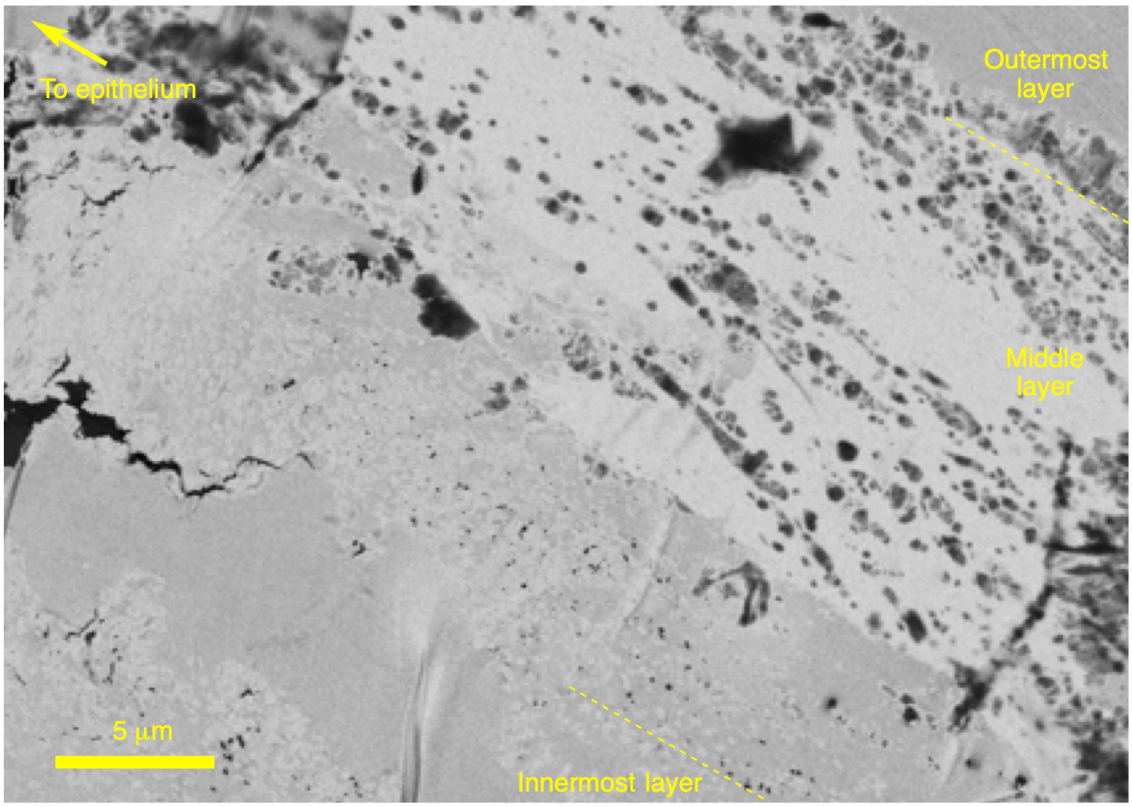

Figure S4. A dark-field STEM image of the cross-section of black scaly-foot scale near the epithelium. Three-layered structures were also observed, although the outermost layer was thinner than that at the tip (Fig. 2a). The particle size at the middle layer was 142 ± 115 nm (*N* = 452 , 37–604 nm range).

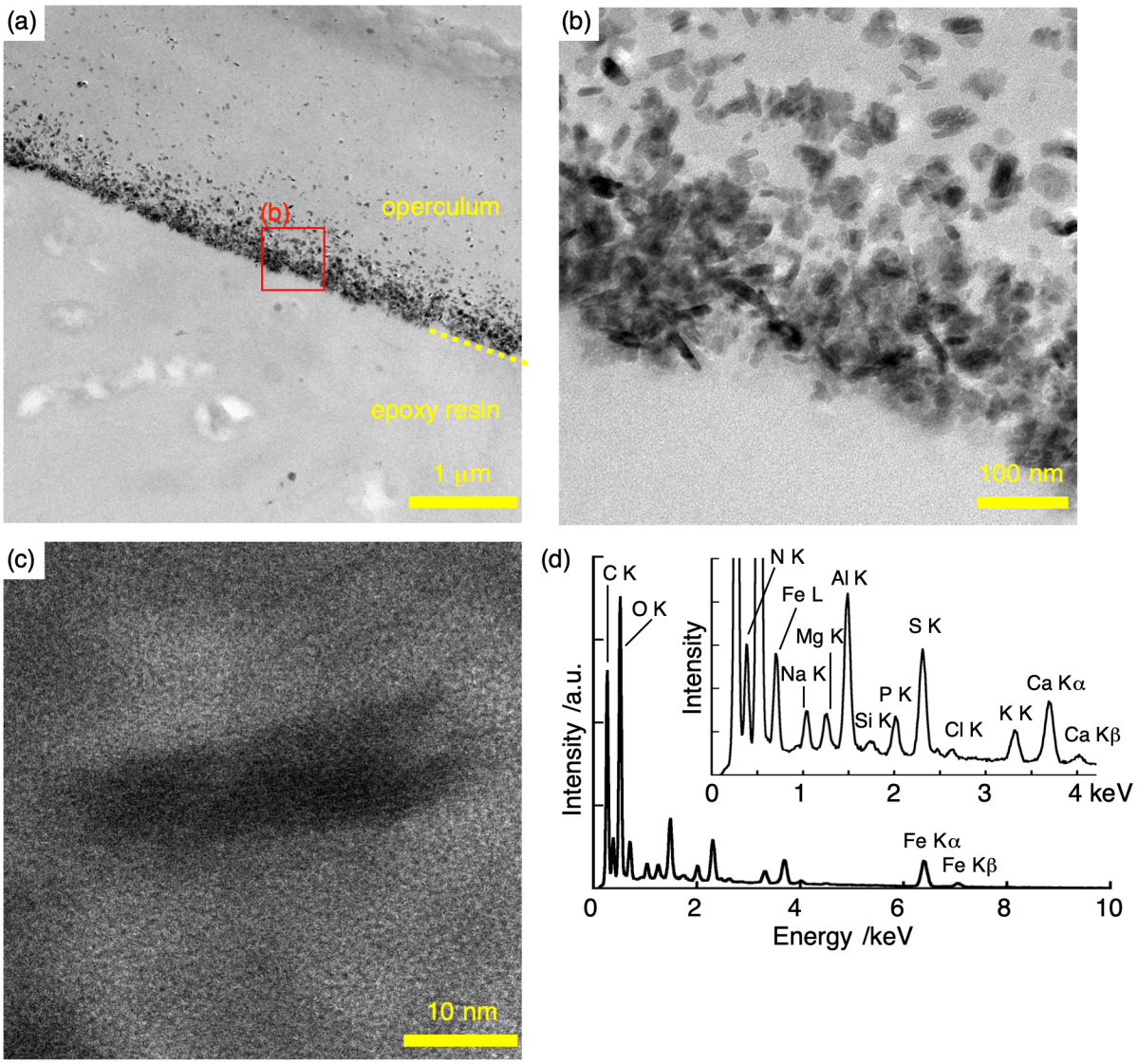

Figure S5. TEM images of the cross-section of the operculum of *Alviniconcha marisindica*. **(a)** A low-magnification image. **(b)** A high-magnification image of the part indicated by a red square in (a). **(c)** A high-resolution image of a single mineral particle observed in (b). **(d)** SEM/EDS spectrum of the surface of the operculum. Imaging and analyses were performed at 200 kV for TEM in (a–c) and 20 kV for SEM/EDS in (d).

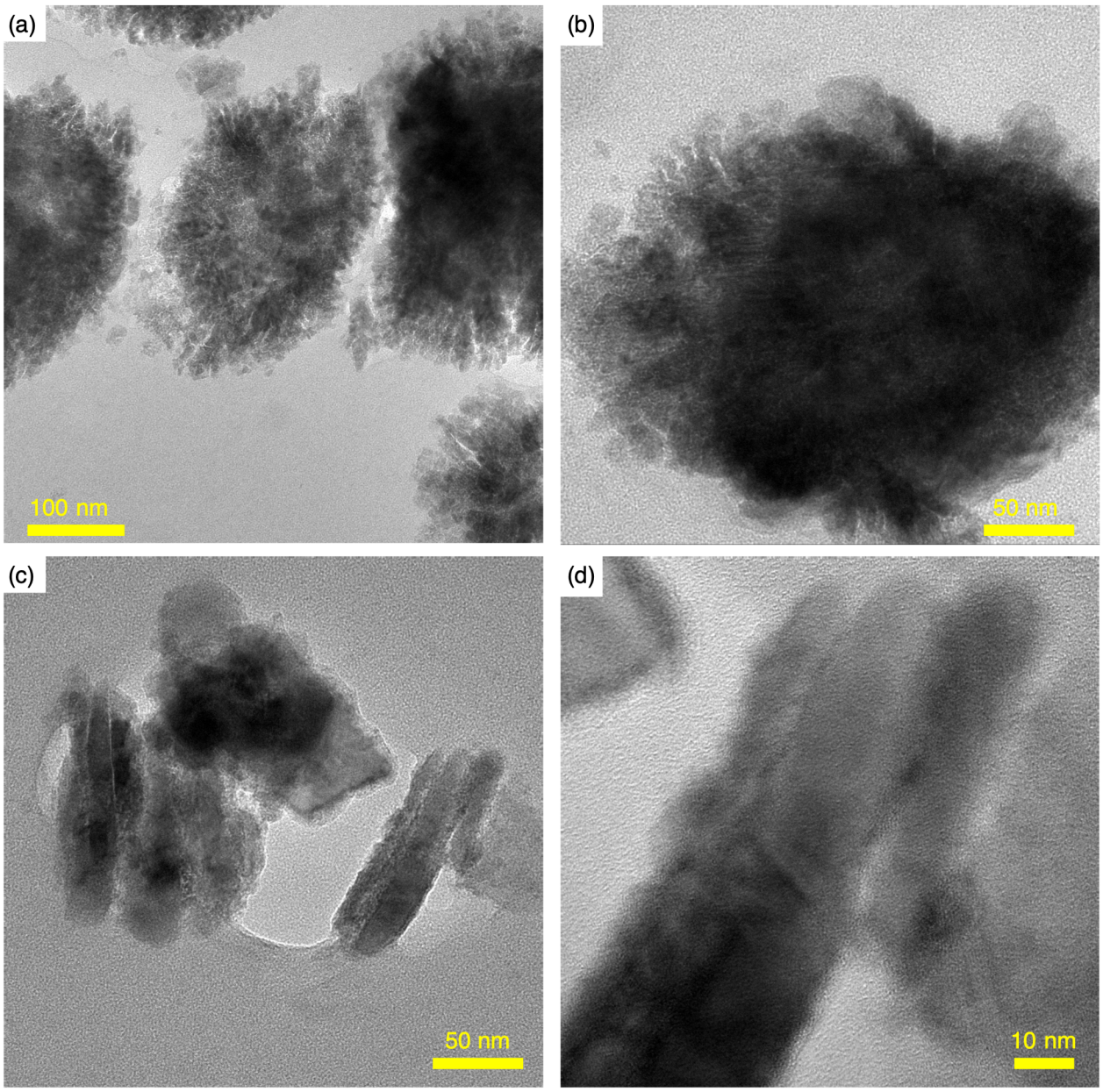

Figure S6. TEM images of nanoparticles in the middle layer of the black scaly-foot scale.

(a, b) Nanoparticle aggregates and (c, d) nanorods. Images are taken at 120 kV.

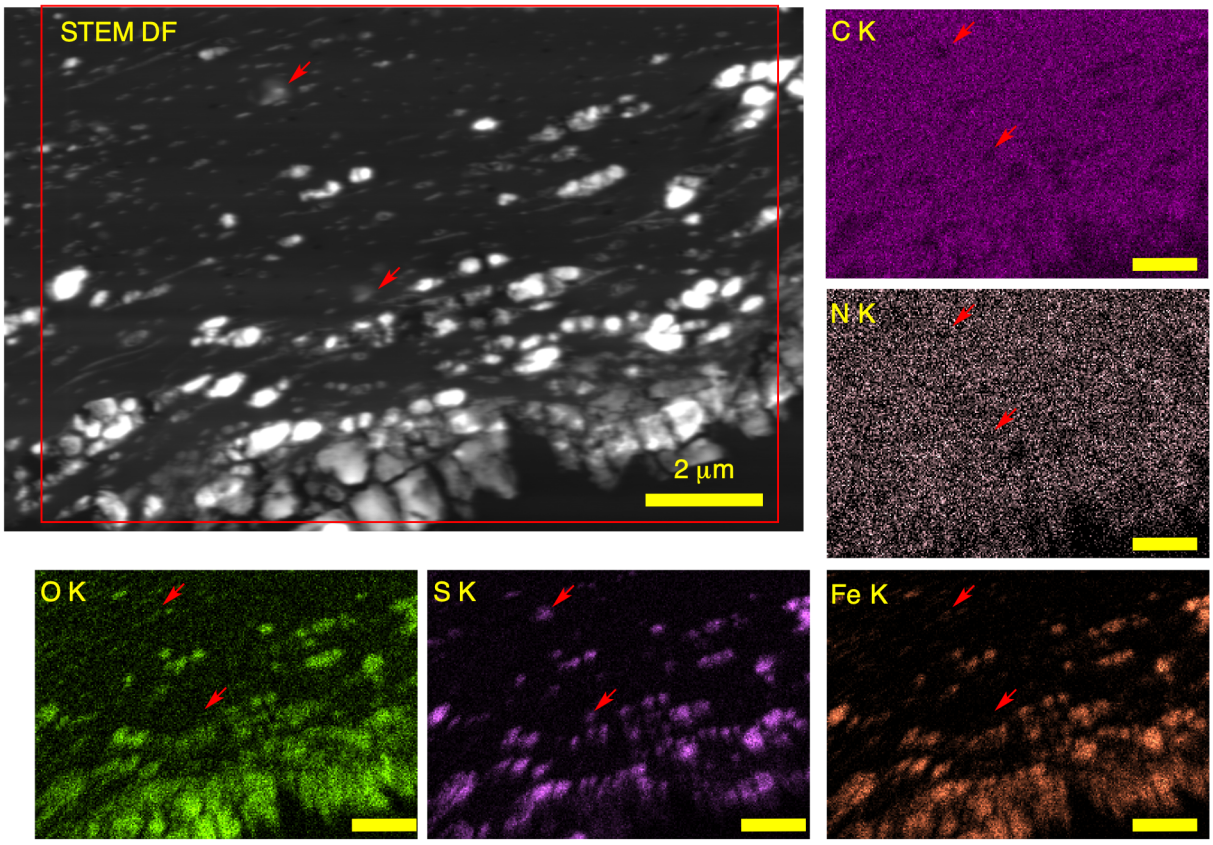

Figure S7. STEM/EDS images of nanoparticles in the black scaly-foot scale. Red square indicates the area analyzed for EDS analyses. Red arrows indicate the sulfur-enriched domain lacking iron. Images were taken at 25 kV. Scale bars, 2 µm.

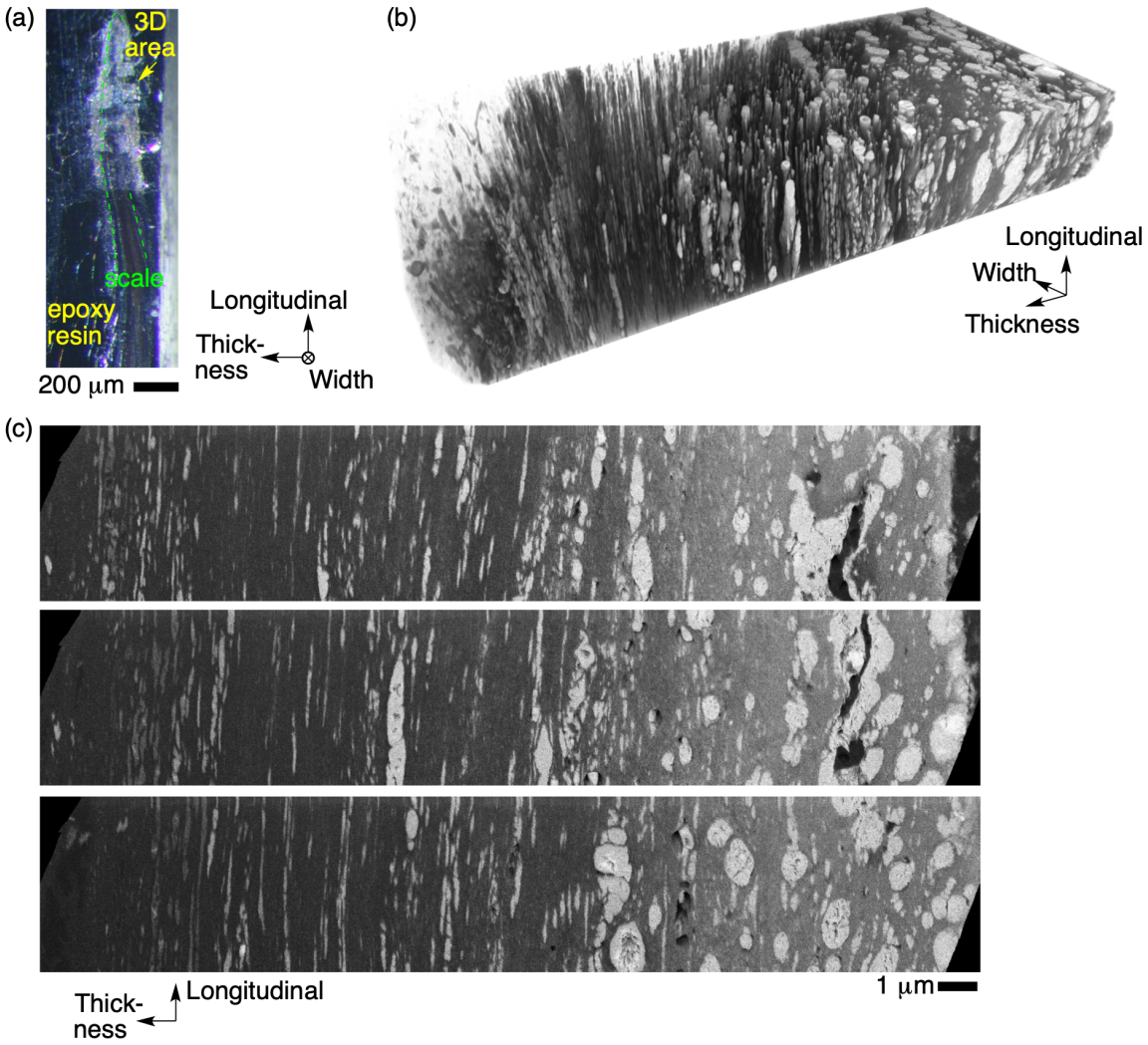

Figure S8. Three-dimensional imaging of a black scaly-foot scale. (a) An optical micrograph of the resin-embedded specimen after carbon coating and FIB-SEM imaging. The green line indicates the periphery of the scale and the yellow arrow indicates the analyzed area. **(b)** Wide-area 3D render showing the channel-like columns. Images were acquired in a solid-state backscattered electron, and the mineralized domains appear in bright contrast. Dark-contrasted tissues were set to transparent to increase visibility of the columns. **(d)** Cross-sectional image of the FIB-SEM slice along the width direction. Imaging was performed at 3 kV. See also supplementary movie 1 for a 3D rotating movie of the rendered image.

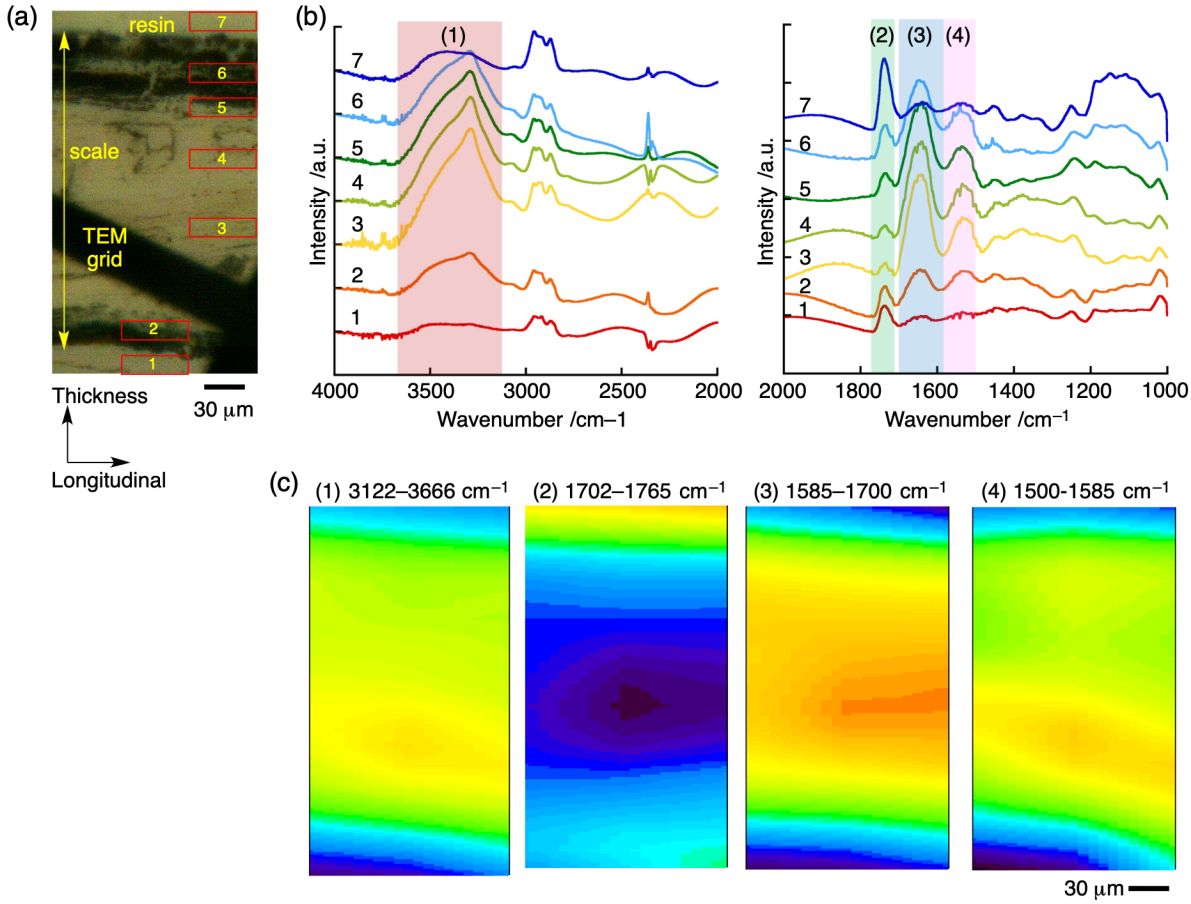

Figure S9. Microscopic infrared mapping image of a black scaly-foot scale. (a) A photomontage of the thin section. **(b)** Infrared spectra of the area indicated by numbered red square in (a). **(c)** Color intensity maps of the colored region in (b); (1) 3122–3666 cm^{-1} corresponds to amide N-H stretching, (2) 1702–1765 cm^{-1} corresponds to ester C=O stretching, (3) 1585–1700 cm^{-1} corresponds to amide C=O stretching, and (d) 1500–1585 cm^{-1} corresponds to amide N-H bending.

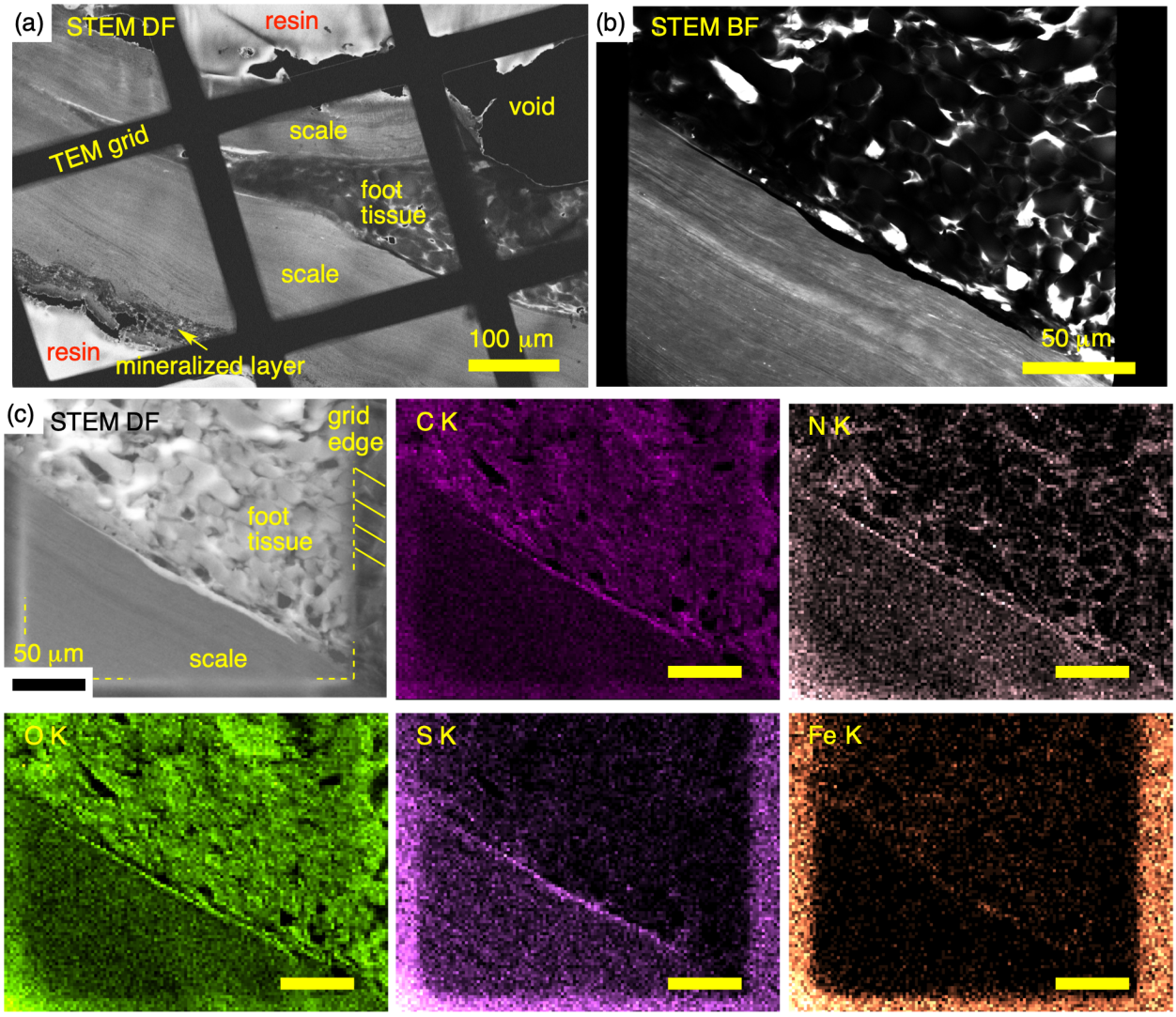

Figure S10. Dark-field STEM images of the interface between the scale and its secreting epithelium in a black scaly-foot scale. (a) A low-magnification image of the thin section. (b) A magnified image of the interface. (c) EDS mapping and (d) EDS spectrum of (b). Imaging and analyses were performed at 25 kV.

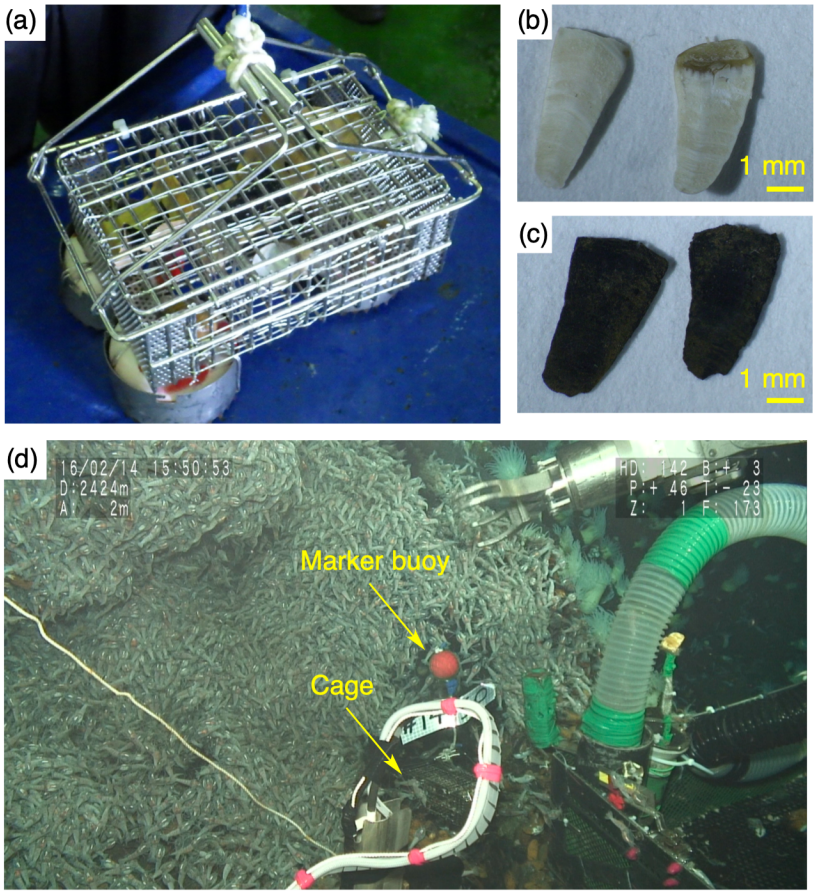

Figure S11. Photographs of the translocation experiment. (a) Scales taken from white scaly-foot were enclosed in a polymer mesh and stored in a metallic cage. **(b)** Scales of white scaly-foot before the translocation experiment. **(c)** The same scales after translocation in Kairei vent field, CIR for 13 days. **(d)** A photograph taken during the translocation experiment. The cage is marked with a red buoy. The chimney is covered by vent shrimps, mostly *Rimicaris kairei*.

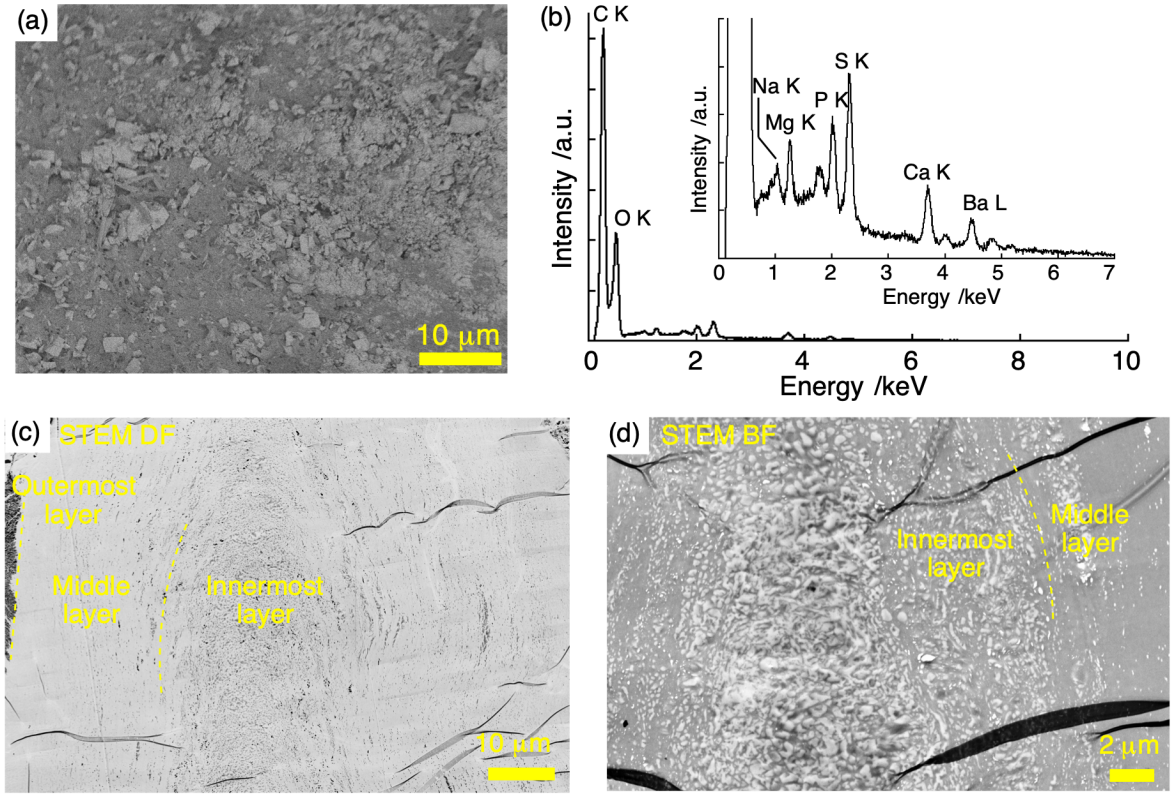

Figure S12. Electron micrographs of white scaly-foot scales. (a) A SEM image of the surface of a white scaly-foot scale. The surface is covered with submicron to micrometer-sized angular particles. **(b)** EDS of (a). Calcium and barium-based minerals were found to be deposited on the surface. **(c)** A STEM image of a thin-section. The same three-layered structure was also observed in white scaly-foot, but lacking minerals within the scale. **(d)** A high-magnification image of the middle and the innermost layers.

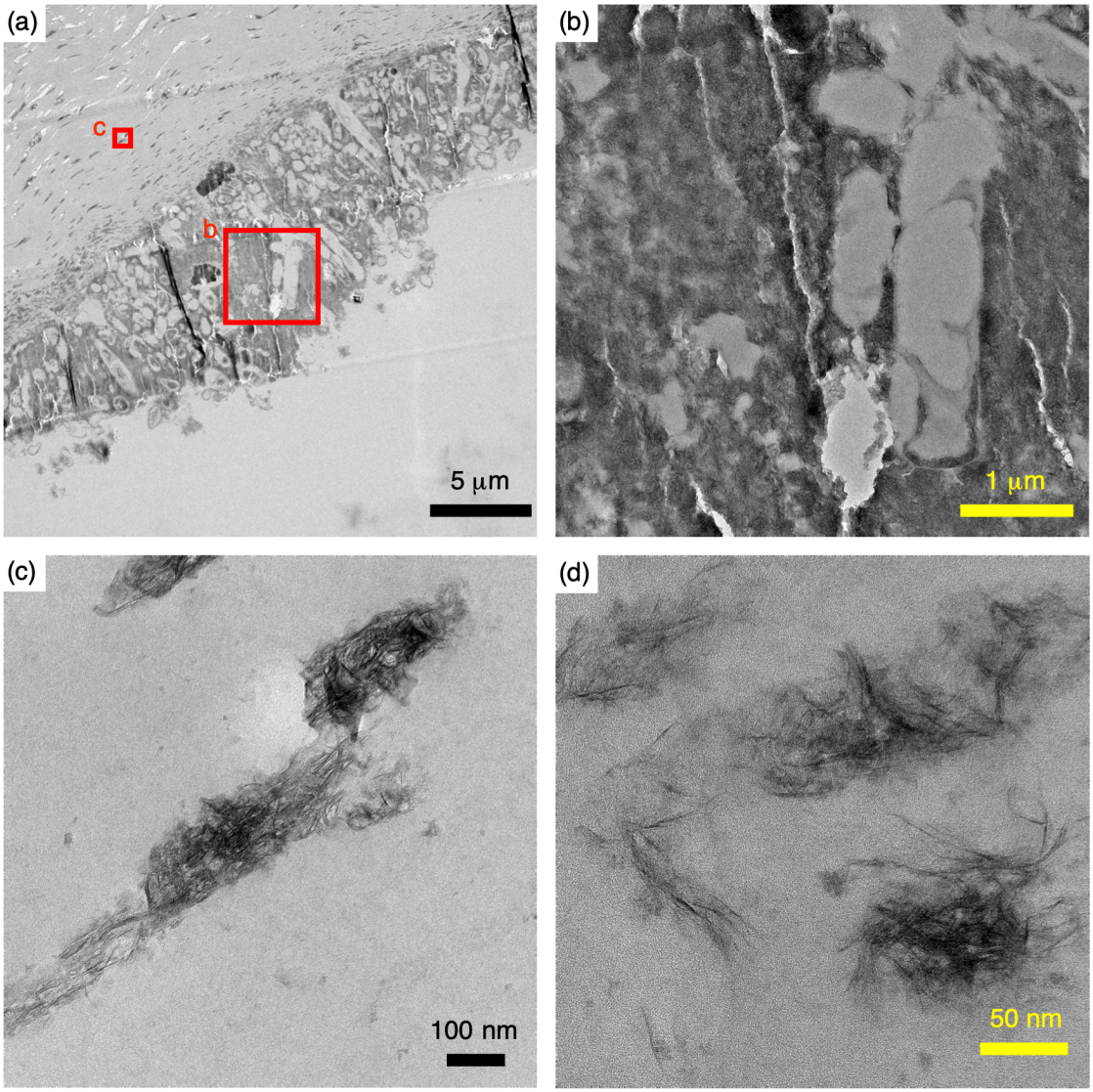

Figure S13. Electron micrographs of translocated scaly-foot scales. (a) A TEM image of the cross section of a translocated scaly-foot scale. **(b, c)** Magnified TEM images of areas indicated by red squares in (a). **(d)** A high-magnification TEM image of the iron sulfide domains. Aggregated flakey minerals with the lattice spacing of 0.7 nm were observed. Images were acquired at 200 kV.

	Position 1			Position 2			Position 3			Position 4		
atom	wt%	atom%	Error	wt%	Atom%	Error	wt%	Atom%	Error	wt%	Atom%	Error
C K	34.76	46.42	9.31	52.37	64.85	9.82	28.66	41.96	10.30	38.28	48.27	9.05
N K	19.22	22.01	11.33	12.94	13.73	15.74	6.58	8.27	13.43	15.89	17.18	12.87
O K	15.95	15.98	11.13	8.85	8.23	14.52	17.36	19.08	10.52	22.65	21.44	11.29
F K	4.17	3.52	19.58	1.38	1.08	35.63	15.14	14.01	13.06	6.37	5.08	26.52
MgK	0.53	0.35	11.43	0.55	0.34	14.83	0.80	0.58	12.32	0.14	0.09	42.57
AlK	12.12	7.20	5.82	18.11	9.98	5.05	15.03	9.79	6.35	11.86	6.66	5.85
SiK	0.08	0.05	37.13	0.28	0.15	23.44	0.20	0.13	23.96	0.00	0.00	99.99
P K	0.15	0.08	21.56	0.49	0.23	15.50	0.19	0.11	23.22	0.02	0.01	99.99
S K	3.65	1.83	3.83	0.78	0.36	11.72	4.94	2.71	4.41	0.18	0.08	21.55
FeK	5.35	1.54	2.80	0.43	0.12	23.40	7.07	2.22	2.70	2.33	0.63	6.86
NiK	0.83	0.23	7.89	1.79	0.45	9.36	1.39	0.42	6.54	0.78	0.20	11.09
CuK	2.96	0.75	4.10	1.87	0.44	10.21	2.48	0.69	5.13	1.50	0.36	9.16
ZnK	0.24	0.06	22.54	0.16	0.04	66.76	0.17	0.05	41.04	0.01	0.00	99.99

Table S1. Elemental composition of Figure S3 (b). Errors are reported in per cent.

	Position 1			Position 2		
atom	wt%	atom%	Error.	wt%	Atom%	Error
C K	57.63	67.19	8.08	77.02	83.79	7.03
N K	8.97	8.97	20.75	5.80	5.41	29.51
O K	17.82	15.60	13.28	7.60	6.21	19.63
F K	4.62	3.40	32.11	1.28	0.88	28.04
MgK	0.35	0.20	17.77	0.23	0.13	24.12
AlK	7.17	3.72	6.01	6.75	3.27	5.32
SiK	0.03	0.01	99.99	0.01	0.01	99.99
P K	0.09	0.04	43.46	0.09	0.04	41.19
S K	0.22	0.10	18.65	0.03	0.01	80.16
ClK	0.12	0.05	30.13	0.07	0.03	67.53
FeK	1.76	0.44	7.23	0.00	0.00	99.99
NiK	0.47	0.11	20.12	0.51	0.11	18.86
CuK	0.75	0.17	17.81	0.60	0.12	22.26

Table S2. Elemental composition of Figure S3 (d). Errors are reported in per cent.

atom	wt%	atom%	Error.
C K	33.57	45.75	9.71
N K	9.71	11.35	12.92
O K	27.51	28.15	10.29
F K	3.96	3.41	23.97
NaK	2.22	1.58	11.71
MgK	0.53	0.36	13.61
AlK	3.47	2.11	6.57
SiK	0.30	0.18	19.83
S K	6.51	3.32	3.13
ClK	1.27	0.59	7.11
FeK	10.95	3.21	3.41
C K	33.57	45.75	9.71
N K	9.71	11.35	12.92

Table S3. Elemental composition of Figure 3 (c). Errors are reported in per cent.

Legends for a Supplementary movie

Movie S1. Three-dimensional imaging of a black scaly-foot scale. Wide-area 3D rotating movie showing the channel-like columns and large granular iron sulfide particles shown in Figure 2e and Supplementary Figure S8. Rotation axis is the longitudinal direction of the scale. Imaging was performed at 3 kV.

References

1. M. Nishizawa, S. Maruyama, T. Urabe, N. Takahata, Y. Sano, Micro-scale (1.5 μm) sulphur isotope analysis of contemporary and early Archean pyrite. *Rapid Commun. Mass Spectrom.* **24**, 1397–1404 (2010).

2. J. H. Luft, Improvements in epoxy resin embedding methods. *J. Biophys. Biochem. Cytol.* **9**, 409–414 (1961).

3. C. Chen, J. T. Copley, K. Linse, A. D. Rogers, J. Sigwart, How the mollusc got its scales: convergent evolution of the molluscan scleritome. *Biol. J. Linnean Soc.* **114**, 949–954 (2015).